Initial design with L^2 Monge-Kantorovich theory for the Monge–Ampère equation method of freeform optics

Rengmao Wu[1], Yaqin Zhang[2], Pablo Benítez[1], and Juan C. Miñano[1]

[1]Universidad Politécnica de Madrid, Cedint, Campus Montegancedo, 28223 Madrid, Spain
[2] State Key Laboratory of modern Optical Instrumentation, Zhejiang University, Hang Zhou 310027, China

ABSTRACT

The Monge–Ampère (MA) equation arising in illumination design is highly nonlinear so that the convergence of the MA method is strongly determined by the initial design. We address the initial design of the MA method in this paper with the L^2 Monge-Kantorovich (LMK) theory, and introduce an efficient approach for finding the optimal mapping of the LMK problem. Three examples, including the beam shaping of collimated beam and point light source, are given to illustrate the potential benefits of the LMK theory in the initial design. The results show the MA method converges more stably and faster with the application of the LMK theory in the initial design.

Keywords: Illumination design, nonimaging optics, freeform surface, computation methods.

1. INTRODUCTION

Illumination design, which controls the distribution of light from a source to produce a target illumination, is a classical problem of nonimaging optics [1]. The traditional method of solving this problem is using the quadric surfaces, such as paraboloid, ellipsoid and spherical surface, to direct the light. The quadric surfaces, though, have been playing an important role in illumination design, the low degree of design freedom of the quadric surfaces, is a frustrating problem faced by the designer. With the increasing emphasis on energy conservation and practical issues, it is becoming a preferred route to solve the problem of illumination design with freeform surface which has higher degree of design freedom [2-11]. The difficulty in the freeform surface illumination design is how to exactly tailor the freeform surface only on the basis of the given intensity distribution of the source and the target illumination. A variety of methods have been developed to solve this problem in the past two decades. The Simultaneous Multiple Surfaces method proposed by Benítez and Miñano allows to simultaneously construct two freeform surfaces that exactly transform two input wavefronts into two output wavefronts [2]. For complex designs, the difficulty of this method lies in establishing a specific relationship between the input and output wavefronts. Optimization method is an iteration of successively finding some appropriate variable values to reduce the merit function value with certain optimization algorithms [3,4]. Due to the Monte-Carlo raytracing and the limited number of optimization variables, the optimization method may not be the best choice in illumination design. The first-order Partial Differential Equation (PDE) method is popular in solving this problem due to its ease of use and fast computation [5,6]. The continuity of the freeform surface designed by the PDE method, however, depends on the integrability of the mapping, and Fournier, using the Supporting Ellipsoids method developed by Oliker [7], has shown the difficulty in obtaining such an integrable mapping [8]. The optimal mass transport also provides an alternative way to get a mapping for freeform surface design [9,10]. Since such a mapping does not include any information about the freeform surface, the mapping may not be integrable and the limitations of these methods in illumination design still need to be further explored [9,10]. The Monge–Ampère (MA) equation method proposed by Ries has shown its elegance in solving the problem of freeform surface illumination [11]. Since the numerical solution of this method was not detailed, this MA method has been covered with a veil of mystery for a long time.

In our previous work [12], we convert the problem of freeform surface illumination design into a nonlinear boundary problem for the elliptic MA equation based on ideal source assumption and introduce an approach to find the numerical sollution of this mathematial problem. By this MA method, the boundary incident rays are mapped to the boundary of the target pattern, and the inner incident rays are pushed to satisfy the elliptical MA equation which describes the conservation and redistribution of energy during the beam-shaping process. Taking the collimated beam shaping for example, the mathematical model of the single freeform surface design is given by [13]

International Optical Design Conference 2014, edited by Mariana Figueiro, Scott Lerner, Julius Muschaweck, John Rogers, Proc. of SPIE-OSA Vol. 9293, 92930M · © 2014 SPIE
CCC code: 0277-786X/14/$18 · doi: 10.1117/12.2072370

$$\begin{cases} A_1(z_{xx}z_{yy}-z_{xy}^2)+A_2z_{xx}+A_3z_{yy}+A_4z_{xy}+A_5=0 \\ BC:\begin{cases} t_x=t_x(x,y,z,z_x,z_y) \\ t_y=t_y(x,y,z,z_x,z_y) \end{cases}:\partial S_1\rightarrow\partial S_2 \end{cases} \tag{1}$$

where, the coefficients which can be written as $A_i=A_i(x, y, z, z_x, z_y)$ (i=1,…,5) are functions of x, y, z, z_x and z_y; t_x and t_y are the x- and y-coordinates of the target point on the illumination plane; ∂S_1 and ∂S_2 represent the boundaries of the domains S_1 of the incident beam and S_2 of the target pattern, respectively. Then, a numerical approach based on the Newton's method is developed to solve this design model (Here, we assume $F_1(\mathbf{X})=0$ represents the nonlinear equations of Eq. (1) obtained by the numerical approach.) [13]. The MA method has shown both mathematical and practical interests in freeform surface illumination design for compact light source and collimated beam [13,14]. The Newton's method which has quadratic convergence is a method for finding better approximations to the roots of a real-valued function. However, for a highly nonlinear function, the convergence of Newton's method is strongly determined by the initial value. The coefficients A_i (i=1,…,4) of the MA equation given in Eq. (1), are usually highly nonlinear in z_x and z_y. Consequently, the convergence of Eq. (1) is strongly determined by the initial design, as illustrated in Fig. 1. The initial design has become one of the most urgent issues to be solved of the MA method in illumination design.

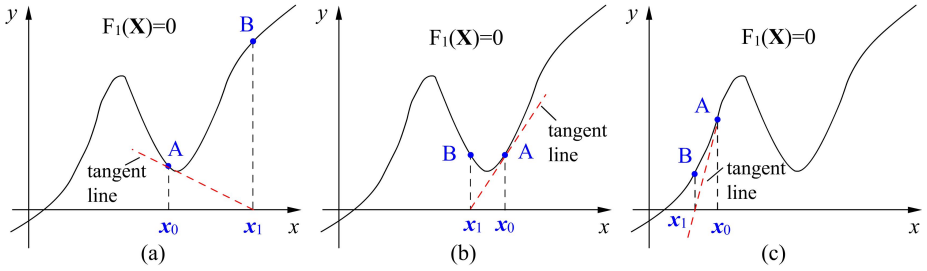

Fig. 1. Some practical considerations for the convergence of the MA method. $\boldsymbol{x}_0$ and $\boldsymbol{x}_1$, respectively, represent the initial value and the x-intercept obtained from the first iteration. (a) The iteration diverges at the first iteration. In this case, $\boldsymbol{x}_1$ may deteriorate the optical performance of the surface. For example, one will uaually encounter complications associated with singularities of the freeform surface, and the method cannot be iterated (This will be demonstrated in the first design example). (b) Assume $F_1(\boldsymbol{x}_0)=F_1(\boldsymbol{x}_1)$ and $|F_1'(\boldsymbol{x}_0)|=|F_1'(\boldsymbol{x}_1)|$. The iteration will go into an infinite loop in this case. (c) $\boldsymbol{x}_0$ may be a good initial guess of a pure mathematical problem in this case. The convergence of the MA method, however, still depends on the optical performance of the freeform surface. For a freeform lens design, the MA method can converge successfully only and if only the total internal reflection will not take place on the freeform surface in the initial design (This will be demonstrated in the second design example).

In order to improve the MA method and promote its application in illumination design, we address the initial design of the MA method in this paper on the basis of the L^2 Monge-Kantorovich (LMK) theory. A new approach of computing a numerical solution of the LMK problem is presented here, and the optimal mapping of this problem is found by solving an equivalent problem not relying on the gradient of time. The approach converges quite fast and is very flexible in imposing the boundary condition. Most importantly, the MA method is significantly improved by applying this new approach to the initial design. The paper is organized as follows. In Section 2, we will review the LMK problem and present an efficient approach to solve the LMK problem. In Section 3, three design examples, including the beam shaping of compact light source and collimated beam, will be given to illustrate the significant improvement of the MA method achieved by the application of the LMK theory in the initial design. Finally, we will conclude with some remarks and discussions in Section 4.

2. L^2 Monge-Kantorovich problem and the new approach

2.1 L^2 Monge-Kantorovich problem

Optimal mass transport is an important problem arising in a number of applications including econometrics, image registration [15], mesh generation [16], automatic control, and reflector design [17]. However, numerical solution of this problem has proved very challenging. The optimal mass transport problem, also known as Monge-Kantorovich problem, can be defined as follows: Let $\rho_0(\boldsymbol{\xi})$ and $\rho_1(\boldsymbol{\eta})$ be two normalized non-negative density functions with compact supports Ω_0 and Ω_1, where $\boldsymbol{\xi}$, $\boldsymbol{\eta}\in R^d$, $d\geq 1$ is the space dimension. Here the data must satisfy the condition that the total mass is conserved:

$$\int_{\Omega_0} \rho_0(\xi) d\xi = \int_{\Omega_1} \rho_1(\eta) d\eta \tag{2}$$

Assume $\phi(\xi)$ is a smooth one-to-one mapping that takes the density $\rho_0(\xi)$ to the density $\rho_1(\eta)$. Then, according to the coordinate transformation between ξ and η, Eq. (2) leads to

$$\det\left(\nabla\phi(\xi)\right)\rho_1\left(\phi(\xi)\right) = \rho_0(\xi) \tag{3}$$

where $\det(\nabla\phi(\xi))$ is the determinant of the Jacobian matrix of the mapping $\phi(\xi)$. The quantity of $\det(\nabla\phi(\xi))$ represents the expansion (or contraction) of an infinitesimal area element of Ω_0 during the mass transport. All the points contained in the infinitesimal area element will converge to a point, a straight line or a curve when $\det(\nabla\phi(\xi))=0$.

There are usually many such mappings which can satisfy Eq. (3), however, there is a unique optimal mapping $\phi = \bar{\phi}$ that minimizes the transport cost

$$C(\phi) = \int_{R^d} \left|\phi(\xi) - \xi\right|^2 \rho_0(\xi) d\xi \tag{4}$$

Moreover, the optimal mapping $\bar{\phi}$ can be expressed as the gradient of a convex function w. That is, $\bar{\phi} = \nabla w$. The infimum of Eq.(4) is the square of the L^2 Kantorovich-Wasserstein distance, and the optimal transport, in this case, is called the L^2 Monge-Kantorovich problem. Substituting $\bar{\phi}$ into Eq.(3), we can find w is a solution of the MA equation

$$\rho_1\left(\nabla w(\xi)\right)\det\nabla^2 w(\xi) = \rho_0(\xi) \tag{5}$$

Here, Eq. (5) is a standard MA equation [18].

2.2 A numerical approach of solving the L^2 Monge-Kantorovich problem

There are two main approaches that can be used to find a numerical solution for Eq. (5). The first one is based on a direct solution of the MA equation [19,20]. The difficulty faced by this approach lies in the discretization of the MA equation. The second approach converts the LMK problem into an evolution problem relying on the gradient of time. For this method, the computational cost may be relevant [15,21]. A numerical method has been presented in Ref. [13] for computing the numerical solution of a kind of elliptic MA equation which is a highly nonlinear MA equation in general form [18]. Based on our previous work, an efficient approach will be introduced here for computing the numerical solution of Eq. (5) in order to obtain an appropriate initial design for the MA method.

Instead of solving Eq. (5) directly, we first establish an equivalent problem of Eq. (5), which is given by

$$\log\left[\rho_1\left(\nabla w(\xi)\right)\det\nabla^2 w(\xi) - \rho_0(\xi) + 1\right] = 0 \tag{6}$$

Note that $\rho_0(\xi)$ is a normalized density function with $\max(\rho_0)=1$ on Ω_0. Then, $\rho_1(\eta)$ is normalized to meet the mass conservation. The value of $\rho_0(\xi)$ could be zero somewhere on Ω_0. That is, $\rho_0(\xi)$ can be a non-negative function, not a strictly positive function. This characteristic is very important for the freeform surface illumination design. We will introduce this characteristic in more detail in Section 3. Eq. (6) represents the conservation and redistribution of mass during the mass transport. Obviously, all the inner points of Ω_0 should satisfy Eq. (6). Then, the boundary conditions (BC) are defined to ensure that all the points on the boundary $\partial\Omega_0$ of Ω_0 are mapped to the boundary $\partial\Omega_1$ of Ω_1. Assume $\partial\Omega_1$ can be represented mathematically by the expression $f(\eta)=0$, then BC will be defined as

$$f\left(\nabla w(\xi)\right) = 0 \qquad \xi \in \partial\Omega_0 \tag{7}$$

Since Eq. (7) does not predefine the specific position of each point on $\partial\Omega_1$, consequently the boundary points can automatically move on $\partial\Omega_1$ until the prescribed transport is achieved. Finally, we obtain an equivalent problem of the LMK problem that is given by

$$\begin{cases} \log\left[\rho_1\left(\nabla w(\xi)\right)\det\nabla^2 w(\xi) - \rho_0(\xi) + 1\right] = 0 & \xi \in \bar{\Omega}_0 \\ BC:\ f\left(\nabla w(\xi)\right) = 0 & \xi \in \partial\Omega_0 \end{cases} \tag{8}$$

where $\Omega_0 = \bar{\Omega}_0 \cup \partial\Omega_0$. In order to find the solution of Eq. (8), we use the discretization scheme introduced in Ref. [13]

to discretize Eq. (8) and get a set of nonlinear equations. Write the nonlinear equations in the form of

$$F_2(\mathbf{Y})=0 \tag{9}$$

and linearize this nonlinear problem using the Newton's method. Further, we can establish an iterative scheme for solving the LMK problem

$$F_2(\mathbf{Y}_k)+F_2'(\mathbf{Y}_k)(\mathbf{Y}_{k+1}-\mathbf{Y}_k)=0 \tag{10}$$

where, $\mathbf{Y}_k$ denotes the solution obtained from the *k-th* iteration and $F'(\mathbf{Y}_k)$ is the Fréchet derivative of F at $\mathbf{Y}_k$. An initial value is needed to initiate the iteration of Eq. (10). In this new approach, the initial value is defined by

$$\mathbf{Y}_0=\frac{1}{2}\left[\bar{X}_{\min}+\frac{x-x_{\min}}{x_{\max}-x_{\min}}\left(\bar{X}_{\max}-\bar{X}_{\min}\right)\right]^2\frac{x_{\max}-x_{\min}}{\bar{X}_{\max}-\bar{X}_{\min}}+\frac{1}{2}\left[\bar{Y}_{\min}+\frac{y-y_{\min}}{y_{\max}-y_{\min}}\left(\bar{Y}_{\max}-\bar{Y}_{\min}\right)\right]^2\times\frac{y_{\max}-y_{\min}}{\bar{Y}_{\max}-\bar{Y}_{\min}} \tag{11}$$

where, $\Omega_{02}=[x_{\min},x_{\max}]\times[y_{\min},y_{\max}]\in R^2$ and $\Omega_{12}=\left[\bar{X}_{\min},\bar{X}_{\max}\right]\times\left[\bar{Y}_{\min},\bar{Y}_{\max}\right]\in R^2$, as shown in Fig. 2. Ω_{02} and Ω_{12} are two rectangular domains which are the minimum rectangles containing Ω_0 and Ω_1, respectively. If $\Omega_0\neq\Omega_{02}$, the density on Ω_{01} (Here, $\Omega_0\cup\Omega_{01}=\Omega_{02}$) is set to be zero. In this case, all the points on Ω_{01} will converge to $\partial\Omega_1$. Equation (11) shows clearly that the target points defined by the initial mapping will uniformly distribute on Ω_{12}. That is, a uniform density distribution can be produced on Ω_{12} by this initial mapping if the density distribution defined on Ω_{02} is uniform. In the next section, we will apply this new approach to the initial design of the MA method.

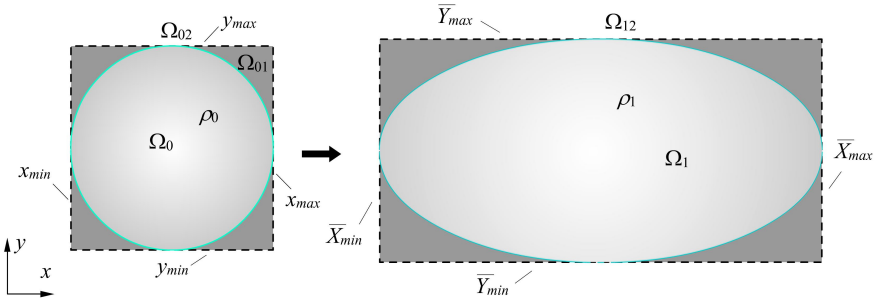

Fig. 2. Define the initial value for the LMK problem.

3. INITIAL DESIGN WITH LMK THEORY

Three examples will be given here to demonstrate the significant improvement of the MA method achieved by applying the LMK theory to the initial design. In the first example, a freeform reflector is required for directing a collimated beam which has a Gaussian intensity distribution with beam waist of 0.3mm. The target is a uniform elliptical pattern and the architecture of the beam shaping system is given in Fig. 3(a). The other parameters are given in Table 1. For ease of description, we use LMA to represent the MA method which utilizes the optimal mapping of the LMK problem in the initial design, and SMA to represent the MA method which dose not utilize the optimal mapping in the initial design.

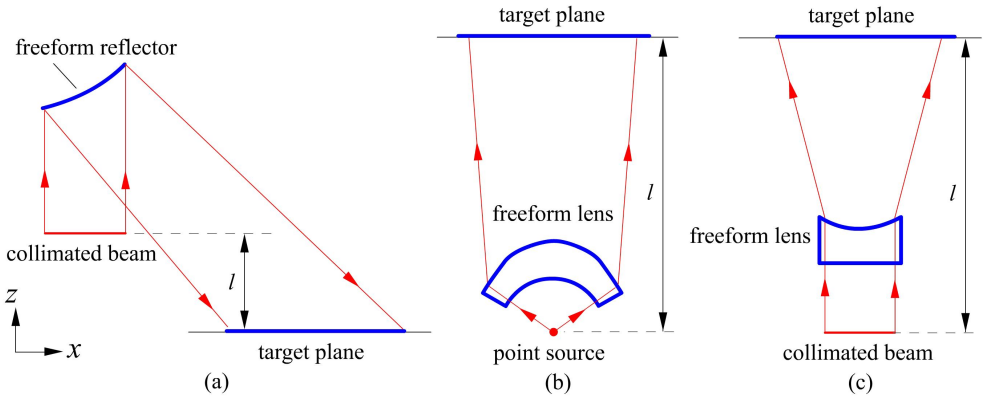

Fig. 3. The architectures of the design examples. *l* denotes the distance between the source and the target plane.

Table 1 Design parameters (unit: millimeter).

	x_{min}	x_{max}	y_{min}	y_{max}	$\bar{X}_{\min}$	$\bar{X}_{\max}$	$\bar{Y}_{\min}$	$\bar{Y}_{\max}$	l
Example 1	-0.5	0.5	-0.5	0.5	6	8	-3	3	10
Example 2	-0.5	0.5	-0.5	0.5	-5	5	-10	10	10
Example 3	-0.5	0.5	-0.5	0.5	-2	2	-2	2	8.2

First, we use the new approach to solve the LMK problem with an initial value defined by Eq. (11), and give the rapid convergence of the LMK problem in Fig. 4(a). After that, we utilize the obtained optimal mapping to design the freeform reflector with PDE method. The illumination pattern produced by the reflector is shown in Fig. 4(b). Since the optimal mapping of the LMK problem does not include any information about the freeform surface, the actual illumination pattern deviates from the target. Then, we use this design as the initial value of the MA method, and find the LMA method converges quite fast, as shown in Fig. 4(c). Obviously, the rapid convergence of the LMA method is achieved by using the initial design obtained from the LMK. Besides, a smooth reflector is obtained and the illumination pattern obtained from the LMA is quite good, as given in Fig. 4(d). We also use a variable separation mapping defined by Eq. (11) to find an initial design for the SMA method. The illumination pattern produced by the initial design is given in Fig. 4(e). From this figure, we observe the pattern deviates significantly from that given in Fig. 4(b), and, of course, deviates significantly from the target. With this initial design, we find the iteration cannot converge. More specifically, we encounter complications associated with singularities of the freeform surface after the first iteration and the iteration stops, as shown in Fig. 4(f). From the comparison made between the two initial designs, we can find the LMK provides a better initial design for the LMA method, which is much closer to the final solution. Besides, from Figs. 4(a) and 4(f) we also observe that although the initial mappings used in the LMK problem and the SMA method are the same, the SMA method cannot converge due to the high nonlinearity of the MA equation.

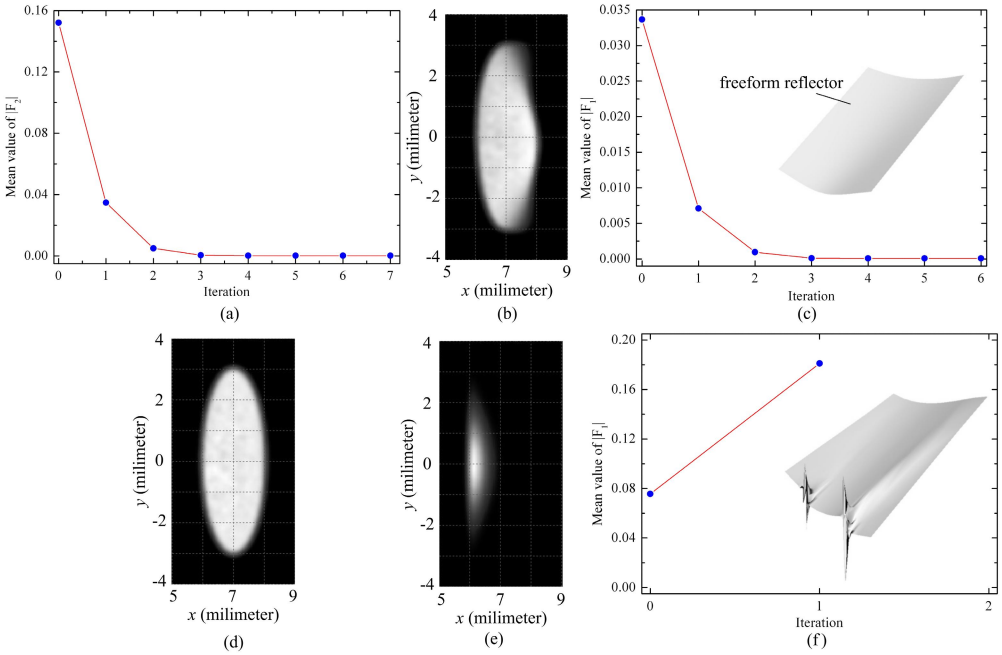

Fig. 4. (a) The convergence of the LMK problem and (b) the illumination pattern obtained from the LMK. (c) The rapid convergence of the LMA method and the obtained smooth reflector, and (d) the illumination pattern obtained from the LMA method. (e) The illumination pattern obtained from a variable separation mapping, (f) the divergence of the SMA method and the singularities of the freeform reflector.

In the second example, a freeform lens is required for beam shaping of a point source. The architecture of the beam shaping system is given in Fig. 3(b). The entrance surface of the lens is a spherical surface, and the light source is located at the centre of curvature of the entrance surface. Assume the refractive index of the freeform lens is 1.59, the light source is a Lambertian source, and the maximum collection angle of the lens equals 120°. The first thing we should do to find the optimal mapping of the LMK problem is to get the projected intensity distribution of the point source on a reference plane. Obviously, such a projected intensity distribution is defined on a circular domain. Based on the new

approach introduced above, the optimal mapping of the LMK problem is found and the initial design of the freeform lens is obtained. The illumination pattern produced by the initial design is given in Fig. 5(a), and the irradiance distribution along the line x=0 mm is depicted in Fig. 5(b). These two figures show clearly that the irradiance distribution obtained from the LMK is not quite uniform, and there is much difference between the obtained distribution and the target. With the initial design, we obtain rapid convergence of the LMA method and a quite good approximate to the solution of the freeform lens design, as shown in Figs. 5(c) and 5(d). Then, we use a mapping given in Fig. 5(e) in the initial design. The illumination pattern produced by the initial design is shown in Fig. 5(f). Obviously, the initial design given in Fig. 5(a) is better than that given in Fig. 5(f), and undoubtedly is closer to the target. Moreover, we also find the SMA method cannot iterate at all even at the first iteration due to the total internal reflection taking place on the freeform surface, as shown in Fig. 5(g).

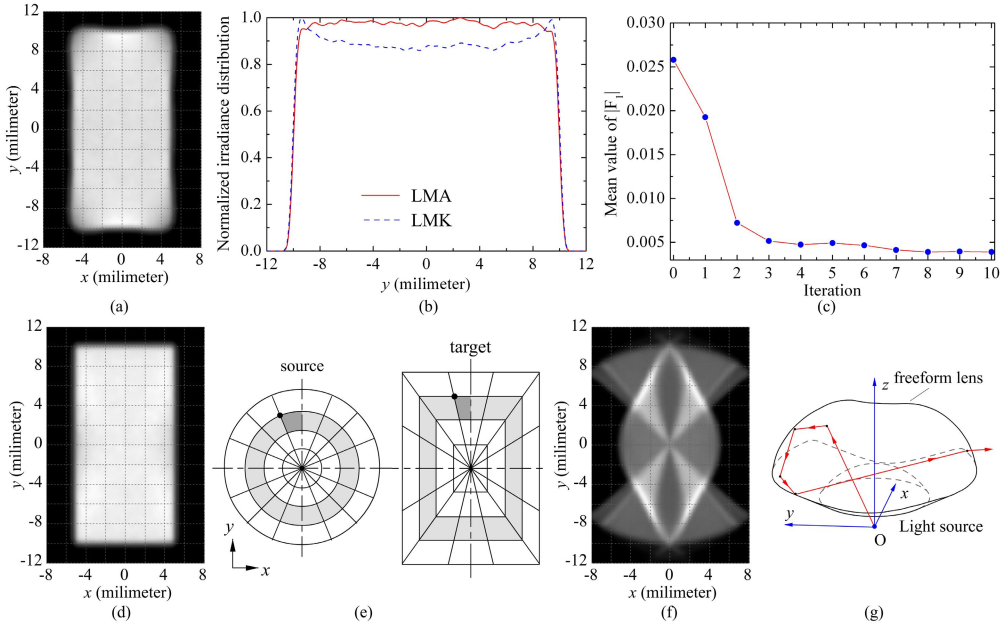

Fig. 5. (a) The illumination pattern obtained from the LMK, and (b) the irradiance curves along the line x=0mm. (c) The rapid convergence of the LMA method and (d) the illumination pattern obtained from the LMA method. (e) A variable separation mapping which is not the optimal mapping of the LMK problem, (f) the illumination pattern produced by the initial design and (g) illustration of the total internal reflection taking place on the freeform surface. The unit vector of the incident ray depicted in (g) is (0.8480,0,0.5299) .

In the last example, a freeform lens is required for solving the following challenging problem of collimated beam shaping. Figure 3(c) gives the layout of the optical system. The intensity of the incident beam is uniform, and the target irradiance distribution should satisfy

$$E(x,y)=\frac{C}{3+\cos\left[2\pi\sqrt{(x-0.7)^2+(y-0.4)^2}\right]} \tag{12}$$

where C is the normalization factor such that Eq. (2) is satisfied. A gray-scale plot of the target distribution is given in Fig. 6(a). Being similar to what we have done in the previous two examples, the first thing is still to use the LMK theory to find an optimal mapping for the initial design. Assume m=n=80. It takes 60.49 seconds to find the optimal mapping. The illumination pattern produced by the initial design is shown in Fig. 6(b). Since the optimal mapping of the LMK problem is not curl-free in this lens design, the obtained irradiance distribution deviates significantly from the target. Being similar to what Bortz and Shatz have done in [22], we also employ the fractional *RMS* to quantify the difference between the actual irradiance distribution and the target:

$$RMS=\sqrt{\frac{1}{M}\sum_{i=1}^{M}\left(\frac{E_{ai}-E_{ti}}{E_{ti}}\right)^2} \tag{13}$$

where, M is the number of the sample points, E_{ti} is the target irradiance of the *i-th* sample point and E_{ai} is the actual irradiance of the *i-th* sample point. A smaller value of *RMS* represents less difference between the actual irradiance distribution and the target. Here, we use 80×80 sample points to compute *RMS*. According to the irradiance distribution, we have *RMS* = 0.3452 for the initial design. Although there is much difference, we can still observe the illumination pattern produced by the initial design is more or less similar to the target.

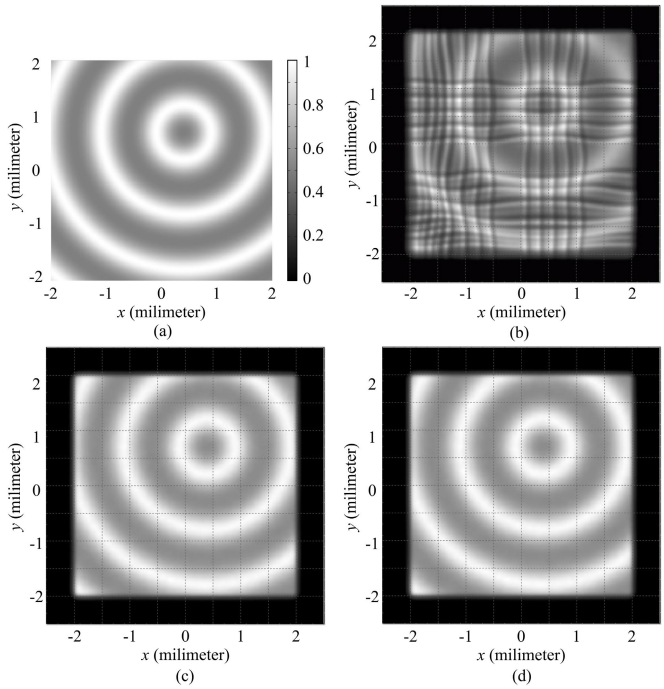

Fig. 6. (a) The target illumination pattern, and the illumination patterns obtained from (b) the LMK, (c) the LMA method and (d) the SMA method.

Assume that $Tol=10^{-11}$ and the iteration stops when $|(\sum|F_{1,i}|-\sum|F_{1,i-1}|)|/N<Tol$. With this initial design obtained from LMK, the LMA method converges quite fast such that the stopping criterion is met after 12 iterations with the computational time of 60.47 seconds, as shown in Fig. 7(a). The irradiance distribution is shown in Fig. 6(c) and we have *RMS* =0.0118. Then, a variable separation mapping defined by Eq. (11) is used here to find the initial design. As mentioned above, the initial design obtained from such a mapping can produce a uniform illumination pattern when the intensity of the incident beam is uniform. With such an initial design, the SMA method also converges and the stopping criterion is met after 18 iterations with the computational time of 94.88 seconds. However, the iteration fluctuates a little bit at the beginning, as shown in Fig. 7(a). The irradiance distribution is shown in Fig. 6(d), and *RMS* =0.0117. Since both the LMA method and the SMA method converge to zero in this design regardless of the numerical errors, there is, of course, little difference between the results of the two methods. Here, we need to point out that the SMA method will not converge at l=8.1mm because we will encounter the complications associated with singularities of the freeform surface, however, the rapid convergence of the LMA method can still be achieved at l=8.1 mm. Since this case have been studied in the first design example, we do not present the details of this case here. The LMA method converges much faster, and figure 7(a) also indicates that the fluctuation can be avoided by using the LMA method. Change l to 10mm, we find the fluctuation of the SMA is eliminated and both the LMA method and the SMA method converge quite fast, as illustrated in Fig. 7(b). The stopping criterion is met after 12 iterations for the LMA method with the computational time of 63.30 seconds and 13 iterations for the SMA method with the computational time of 73.89 seconds, respectively. Figure 7(a) shows that the stopping criterion is also met after 12 iterations for the LMA method at l=8.2 mm. This indicates that the convergence of the LMA method is more stable and faster than that of the SMA method.

Although the optimal mapping of the LMK problem may not satisfy the integrability condition in freeform surface illumination design, the optimal mapping is indeed a better option for the initial design of the MA method. The three design examples presented above clearly show that the MA method converges more stably and faster with the application of the LMK theory in the initial design.

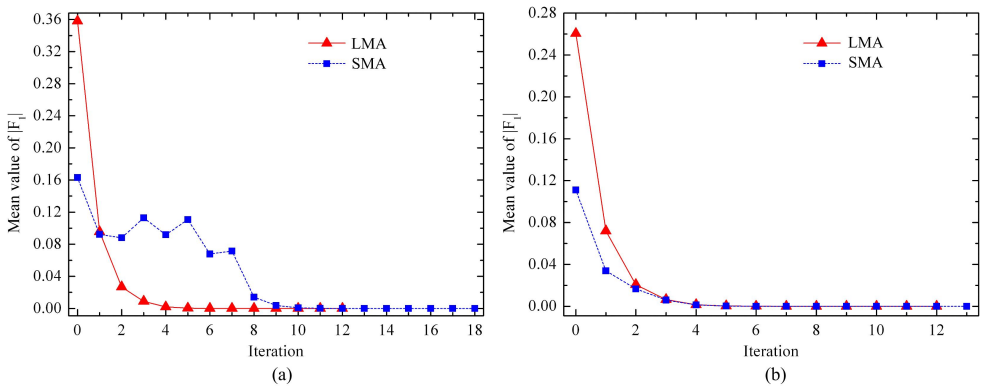

Fig. 7. Illustration of the convergence of the LMA method and the SMA method at (a) *l*=8.2mm and (b) *l*=10mm.

4. CONCLUSION

Due to high nonlinearity of the MA equation, the convergence of the MA method is strongly determined by the initial design. In this paper, we address the initial design of the MA method with the LMK theory. Instead of finding the direct solution of the LMK problem or converting the LMK problem into an evolution problem, we introduce an efficient approach by which the LMK problem is converted into an equivalent problem without relying on the gradient of time. The rapid convergence of this new approach is illustrated. The optimal mapping of the LMK problem, though, is not curl-free in illumination design, it may still be a good option in the initial design of the MA method. Three design examples, including the beam shaping of collimated beam and point light source, are presented to illustrate the potential benefits of the LMK theory in the initial design of the MA method. Detailed comparisons are made between two different initial designs: one is obtained from the optimal mapping of the LMK problem, and the other one is obtained from the variable separation mapping which is usually used in illumination design. The results clearly show the MA method converges more stably and faster with an initial design obtained from the LMK theory. Moreover, the new approach presented here can also be applied to some other methods of freeform surface illumination design which rely on the initial value.

ACKNOWLEDGMENT

This work was carried out during the tenure of an ERCIM "Alain Bensoussan" Fellowship Programme. The research leading to the results has received funding from the European Union Seventh Framework Programme (FP7/2007-2013) under grant agreement n° 246016. Authors thank the European Commission (SMETHODS: FP7-ICT-2009-7 Grant Agreement No. 288526, NGCPV: FP7-ENERGY.2011.1.1 Grant Agreement No. 283798), the Spanish Ministries (ENGINEERING METAMATERIALS: CSD2008-00066, SEM: TSI-020302-2010-65 SUPERRESOLUCION: TEC2011-24019, SIGMAMODULOS: IPT-2011-1441-920000, PMEL: IPT-2011-1212-920000), and UPM (Q090935C59) for the support given to the research activity of the UPM-Optics Engineering Group, making the present work possible.

REFERENCE

1. R. Winston, J. C. Miñano, and P. Benítez, with contributions by N. Shatz and J. C. Bortz, *Nonimaging Optics* (Elsevier, 2005).
2. P. Benítez, J. C. Miñano, J. Blen, R. Mohedano, J. Chaves, O. Dross, M. Hernández, and W. Falicoff, "Simultaneous multiple surface optical design method in three dimensions," Opt. Eng. **43**, 1489–1502 (2004).
3. T. L. R. Davenport, T. A. Hougha, and W. J. Cassarlya, "Optimization for illumination systems: the next level of design," Proc. SPIE **5456**: 81-90 (2004).
4. F. Fournier and J. Rolland, "Optimization of freeform lightpipes for light-emitting-diode projectors," Appl. Opt. **47**, 957-966 (2008).
5. L. Wang, K. Y. Qian, and Y. Luo, "Discontinuous free-form lens design for prescribed irradiance," Appl. Opt. **46**, 3716–3723 (2007).
6. Y. Ding, X. Liu, Z. R. Zheng, and P. F. Gu, "Freeform LED lens for uniform illumination," Opt. Express **16**, 12958–12966 (2008).

7. V. I. Oliker, “Mathematical Aspects of Design of Beam Shaping Surfaces in Geometrical Optics,” in *Trends in Nonlinear Analysis*, M. Kirkilionis, S. Krömker, R. Rannacher and F. Tomi, eds. (Springer Verlag, 2000), pp. 193-224.
8. F. R. Fournier, W. J. Cassarly, and J. P. Rolland, “Fast freeform reflector generation using source-target maps,” Opt. Express **18**, 5295–5304 (2010).
9. A. Bruneton, A. Bäuerle, R. Wester, J. Stollenwerk, and P. Loosen, “High resolution irradiance tailoring using multiple freeform surfaces,” Opt. Express **21**, 10563-10571 (2013)
10. Z. X. Feng, L. Huang, M. L. Gong, and G. F. Jin, “Designing double freeform optical surfaces for controlling both irradiance and wavefront,” Opt. Express **21**, 28693-28701 (2013).
11. H. Ries and J. Muschaweck, “Tailored freeform optical surfaces,” J. Opt. Soc. Am. A **19**, 590-595 (2002).
12. R. M. Wu, L. Xu, P. Liu, Y. Q. Zhang, Z. R. Zheng, H. F. Li, and X. Liu, “Freeform illumination design: a nonlinear boundary problem for the elliptic Monge–Ampère equation,” Opt. Lett. **38**, 229-231 (2013).
13. R. M. Wu, P. Liu, Y. Q. Zhang, Z. R. Zheng, H. F. Li, and X. Liu, “A mathematical model of the single freeform surface design for collimated beam shaping,” Opt. Express **21**, 20974-20989 (2013).
14. R. M. Wu, K. Li, P. Liu, Z. R. Zheng, H. F. Li, and X. Liu, “Conceptual design of dedicated road lighting for city park and housing estate,” Appl. Opt. **52**, 5272-5278 (2013).
15. S. Haker, L. Zhu, A. Tannenbaum, and S. Angenent, “Optimal mass transport for registration and warping,” Int. J. of Comput. Vision. **60**, 225–240 (2004).
16. G. L. Delzanno, L. Chacon, J. M. Finn, Y. Chung, and G. Lapenta, “An optimal robust equidistribution method for two-dimensional grid adaptation based on Monge-Kantorovich optimization,” J. Comput. Phys. **227**, 9841-9864 (2008).
17. T. Glimm and V. I. Oliker, “Optical design of single reflector systems and the Monge-Kantorovich mass transfer problem,” J. Math. Sci. **117**, 4096–4108 (2003).
18. N. S. Trudinger, X.-J. Wang, “The Monge-Ampère equations and its geometric applications,” in *Handbook of Geometric Analysis*, (International Press, 2008), pp. 467-524.
19. E. J. Dean; R. Glowinski, “Numerical methods for fully nonlinear elliptic equations of the Monge Ampere type,” Computer Methods in Applied Mechanics and Engineering, **195**, 1344–1386 (2006).
20. B. D. Froese, “A numerical method for the elliptic Monge-Ampere equation with transport boundary conditions,” SIAM Journal on Scientfic Computing, **34**, A1432-A1459 (2012).
21. M. M. Sulman, J. F. Williams, and R. D. Russell, “An efficient approach for the numerical solution of Monge-Ampère equation,” Appl. Numer. Math. 61, 298–307 (2011).
22. J. Bortz and N. Shatz, “Iterative generalized functional method of nonimaging optical design,” Proc. SPIE **6670**, 66700A (2007).